

Groundwater Seepage Vectors and the Potential for Hillslope Failure and Debris Flow Mobilization

RICHARD M. IVERSON AND JON J. MAJOR

U.S. Geological Survey, David A. Johnston Cascades Volcano Observatory, Vancouver, Washington

Insight for understanding the effect of groundwater flow on the potential for hillslope failure and liquefaction is provided by a novel limit-equilibrium analysis of infinite slopes with steady, uniform Darcian seepage of arbitrary magnitude and direction. Normalization of the limit-equilibrium solution shows that three dimensionless parameters govern completely the Coulomb failure potential of saturated, cohesionless, infinite homogeneous hillslopes: (1) the ratio of seepage force magnitude to gravitational body force magnitude; (2) the angle $\theta - \phi$, where θ is the surface slope angle and ϕ is the angle of internal friction of the soil; and (3) the angle $\lambda + \phi$, where λ is the angle of the seepage vector measured with respect to an outward-directed surface-normal vector. An additional dimensionless parameter affects the solution if soil cohesion is included in the analysis. Representation of the normalized solution as a single family of curves shows that minimum slope stability universally occurs when the seepage direction is given by $\lambda = 90^\circ - \phi$. It also shows that for some upward seepage conditions, slope stability is limited by static liquefaction rather than by Coulomb failure. Close association between these liquefaction conditions and certain Coulomb failure conditions indicates that slope failure in such instances could be responsible for nearly spontaneous mobilization of destructive flowing soil masses on hillslopes.

INTRODUCTION

The important influence of groundwater seepage on the effective stress state and stability of soil masses has long been recognized. Two simple examples of the effect of steady groundwater seepage on the stability of a static semi-infinite soil mass bounded by a free surface are almost universally presented in soil mechanics texts [e.g., *Lambe and Whitman, 1979, p. 263-264, 352-354*]: (1) a cohesionless saturated soil mass will statically liquefy to a quick condition if it is subject to an upward seepage force equal in magnitude to the submerged unit weight of the soil, and (2) the maximum stable angle of a sloping mass of water-saturated cohesionless soil is equal to the internal friction angle of the soil if seepage is absent, but it is equal to about half this angle if uniform slope-parallel seepage occurs. These maxims are true regardless of the magnitudes of the pore water pressures involved. Such simple examples of steady seepage effects are very useful because they convey clearly the influence of groundwater flow on the potential for slope instability. These simple examples are not, however, representative of most field situations [*Patton and Hendron, 1974; Hodge and Freeze, 1977*], and they exclude many important combinations of soil stress states and seepage paths.

More realistic steady seepage conditions are commonly investigated by manually or computationally constructing a flow net [e.g., *Lambe and Whitman, 1979, pp. 266-280*]. The flow net is used to deduce the distribution of seepage forces or pore pressures in the soil mass, and this distribution can then be employed in a slope-stability analysis. The flow net method may be quite accurate, but it is typically problem-specific. It does not clarify the general physical significance of steady seepage effects on the potential for slope instability.

In this paper we derive a simple but general analytical solution for the limiting stable slope angle of a semi-infinite, homogeneous, isotropic cohesionless soil mass subject to steady, uniform Darcian seepage. A normalized solution is developed

for any combination of seepage rate and direction, soil bulk density, pore fluid density, slope angle, and soil friction angle. The results apply to all possible modes of Coulomb failure or liquefaction of static saturated soil masses. The results can be extended to include the effects of soil cohesion, but they do not account for unsteady groundwater flow or soil consolidation. In effect, the results provide a complete and unambiguous answer to the question, If all else is constant, what is the effect of a steady seepage vector (i.e., its magnitude and direction) on the potential for slope failure and liquefaction?

We believe these results provide considerable insight for understanding the physical effects of groundwater flow on the potential for slope instability and debris flow mobilization. Furthermore, the analytical results can guide interpretation of field data and numerical modeling results. Examples of simple applications are included at the end of the paper.

ANALYSIS OF COULOMB FAILURE

To give the slope failure analysis a sound theoretical basis we will start from fundamental stress-equilibrium principles and then simplify to equations of limiting equilibrium. Consider a differential volume element of rigid, homogeneous, isotropic, isothermal soil that is subject to body forces caused by gravity and a steady, uniform Darcian flow field. Static equilibrium of the solid constituents of the soil element requires that [*Iverson, 1986a, equations 2 and 5*]

$$\mathbf{V} \cdot \mathbf{T} = (\rho_t - \rho_w)\mathbf{g} + \mathbf{f} \quad (1)$$

in which \mathbf{T} is the effective stress tensor (with normal stress defined as positive in compression); ρ_t and ρ_w are the total soil bulk density and pore water density, respectively; \mathbf{g} is the gravitational acceleration vector; and \mathbf{f} is the seepage-force vector. The seepage force experienced by the solid constituents of the soil element is proportional to the specific discharge (volumetric flux per unit area) of groundwater flowing through the element [e.g., *Bear, 1972, p. 184-186*]. This can be easily seen from an inverted form of Darcy's law

$$\mathbf{f} = (\mathbf{q}/K)\rho_w\mathbf{g} = -\rho_w\mathbf{g}\nabla h \quad (2)$$

in which g is the magnitude of \mathbf{g} , h is the total hydraulic head

This paper is not subject to U.S. copyright. Published in 1986 by the American Geophysical Union.

Paper number 6W4423.

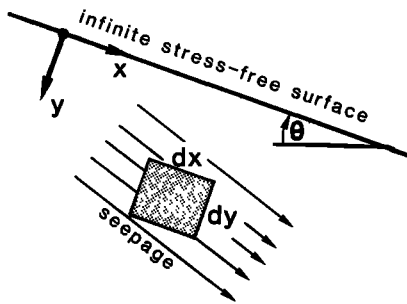


Fig. 1. Differential element in a saturated semi-infinite soil mass with uniform seepage of arbitrary magnitude and direction.

of the pore water, q is the specific discharge vector, and K is the hydraulic conductivity, which is a scalar quantity for isotropic soil. Consideration of the seepage force acting through a soil element appears to us to be the most illuminating way to consider groundwater influences on effective stresses in soils. The seepage force definition accounts implicitly for the mechanical energy or head losses implied by Darcy's law for isothermal flow, and it is intimately linked to the Darcian assumptions of element-averaged groundwater discharge and hydraulic conductivity.

If the differential soil element is assumed further to lie within a semi-infinite mass of identical soil that is bounded by a stress-free surface, and if the only forces affecting the soil are those due to the steady homogeneous vector fields that represent gravitational acceleration and Darcian seepage, then stress gradients do not exist in planes parallel to the stress-free boundary. Thus stresses vary in only the y direction if the global, orthogonal coordinate system of Figure 1 is adopted. Seepage components perpendicular to the vertical x - y plane of Figure 1 exert no forces that can interact with gravitational forces to influence slope stability. Seepage will therefore be treated as though it were confined exclusively to the x - y plane (Figure 1), with no resulting loss of physical generality. The vector equations (1) and (2) can then be combined and reduced to two scalar equations for the sole nonvanishing gradients of hydraulic head and stress

$$d\sigma/dy = \gamma_b \cos \theta - (\partial h/\partial y)\gamma_w \tag{3a}$$

$$d\tau/dy = \gamma_b \sin \theta - (\partial h/\partial x)\gamma_w \tag{3b}$$

where σ is effective normal stress in the y direction; τ is shear stress in the x direction on planes normal to y ; $\gamma_b = (\rho_t - \rho_w)g$, $\gamma_w = \rho_w g$; and θ is the slope angle of the soil surface, which is measured clockwise from the horizontal and assumed to lie in the range $0 < \theta < 90^\circ$. (The angle θ , of course, would be measured counterclockwise if the observer were looking outward from the plane of Figure 1.) Equations (3) can be recast in terms of pore water pressure gradients and the total unit weight of the soil (appendix), but the notion of a seepage force vector proves useful in the following analysis, so the forms of (3) will be retained.

The condition of limiting equilibrium or incipient frictional failure for a cohesionless soil is approximated well by the Coulomb equation [Lambe and Whitman, 1979, p. 139]

$$\tau = \sigma \tan \phi \tag{4}$$

in which ϕ is the static angle of internal soil friction. For a soil element subject to the one-dimensional stress field and uniform Darcian flow field represented by (3), (4) is satisfied

everywhere in the element if it is satisfied anywhere in the element. In other words, the element will in theory fail simultaneously throughout its thickness. No information is therefore lost from (4) if it is differentiated with respect to y

$$d\tau/dy = (d\sigma/dy) \tan \phi \tag{5}$$

Equation (3) can then be substituted into (5) to give

$$\tan \phi = \frac{\gamma_b \sin \theta - \gamma_w(\partial h/\partial x)}{\gamma_b \cos \theta - \gamma_w(\partial h/\partial y)} \tag{6}$$

which applies under conditions of limiting equilibrium or incipient yield.

Equation (6) can be expressed in a more convenient form by defining an angular direction and magnitude of the hydraulic gradient vector. As is shown in Figure 2, the angular direction λ of the hydraulic gradient or seepage vector is measured clockwise relative to an outward-directed vector that is normal to the ground surface. (Again, this angle would be measured counterclockwise if the observer were looking outward from the plane of the page.) The magnitude of the hydraulic gradient or seepage vector i is equal to the magnitude of the change in head per unit length along a flow line. Therefore i is equal to the magnitude of specific discharge divided by the hydraulic conductivity. It follows directly from the definition of λ in Figure 2 that

$$\partial h/\partial x = -i \sin \lambda \tag{7a}$$

$$\partial h/\partial y = i \cos \lambda \tag{7b}$$

Employing (7), (6) can be expressed in the convenient form

$$\tan \phi = \frac{[(\gamma_t/\gamma_w) - 1] \sin \theta + i \sin \lambda}{[(\gamma_t/\gamma_w) - 1] \cos \theta - i \cos \lambda} \tag{8}$$

in which γ_t is the total saturated unit weight of the soil.

Equation (8) is an implicit solution for the limiting stable slope angle θ of a semi-infinite mass of cohesionless soil subject to seepage in the direction λ and driven by a gradient of magnitude i . A plot of the solution of (8) for a typical sandy soil, with $\phi = 30^\circ$, $\gamma_t/\gamma_w = 2$, and selected values of i is shown in Figure 3. The curves of Figure 3 are plotted for only those combinations of θ , λ , and i that appear to be most plausible in nature. The curves are not shown where unlikely combinations of θ , λ , and i occur, for example, where $\lambda < 0^\circ$ (implying an uphill seepage component), $\theta > 60^\circ$ (implying an unrealistically steep slope), or $i > 1$ (implying an unusually large hydraulic gradient). Curves of the type shown in Figure 3 provide a guide for estimating the role of groundwater flow in provoking slope failure in specific situations.

A universally applicable family of Coulomb failure curves similar to those shown in Figure 3 can be obtained from a normalized version of (8). The normalized equation is obtained by expressing $\tan \phi$ in (8) as $\sin \phi/\cos \phi$ and cross-

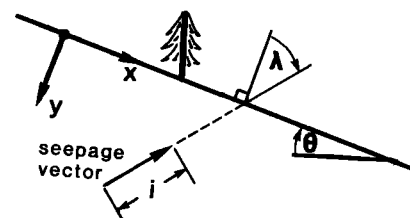


Fig. 2. Definition of the seepage vector magnitude and direction.

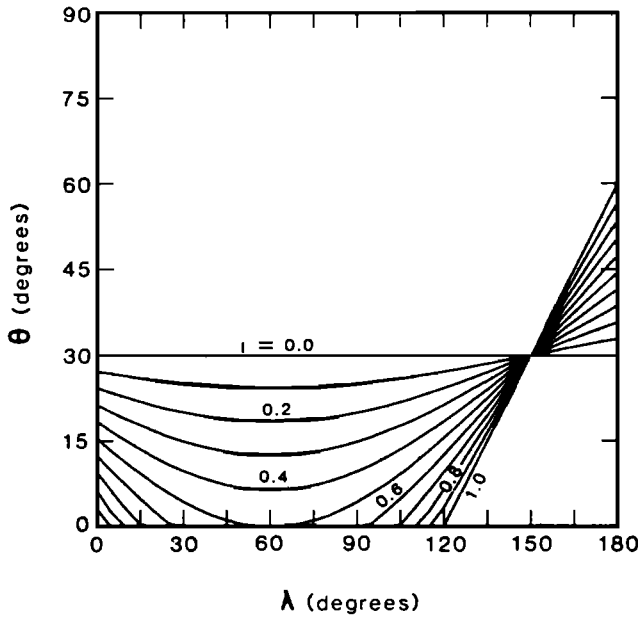


Fig. 3. Plot of limiting stable slope angle θ as a function of seepage direction λ for different seepage magnitudes for a typical sandy soil ($\phi = 30^\circ, \gamma_t/\gamma_w = 2$).

multiplying the numerators and denominators of the resulting equation. This yields, after some algebraic manipulation

$$\frac{\sin \phi \cos \theta - \sin \theta \cos \phi}{\sin \phi \cos \lambda + \sin \lambda \cos \phi} = \frac{i\gamma_w}{\gamma_t - \gamma_w} \quad (9)$$

Trigonometric identities tabulated by Dwight [1961, equations 401.01 and 401.02] are then employed to reduce (9) to

$$-\sin(\theta - \phi)/\sin(\lambda + \phi) = z \quad (10)$$

in which

$$z = i\gamma_w/(\gamma_t - \gamma_w) \quad (11)$$

Therefore z presents the ratio of seepage force magnitude to the submerged unit weight of the soil, a quantity that is clearly of fundamental importance. The arguments of the sine functions in equation (10) are also of fundamental importance: they are the "natural" normalized angles that dictate the limits of stability of ideal, cohesionless saturated slopes with uniform Darcian seepage.

A plot of the solution of (10) for parameter values that reflect any physically realizable Coulomb failure condition for ideal, cohesionless saturated slopes is depicted by the family of curves in Figure 4. The minima of all curves occur where $\lambda = 90^\circ - \phi$, indicating that this seepage direction universally yields minimum slope stability. Conversely, seepage in the direction $\lambda = 270^\circ - \phi$ gives maximum slope stability, and seepage in the direction $\lambda = 180^\circ - \phi$ has no effect on stability, regardless of the value of z . Some portions of the curves shown in Figure 4 would be rather unlikely to occur in nature, but they are included for conceptual completeness. A movable discontinuity would exist in all curves on the line where $\theta = 0$, because Coulomb failure would there be impossible. A bound for the failure curves is provided by lines that represent the condition of $z = 1$ and $\theta = -\lambda$. This is the condition of static soil liquefaction caused by upward groundwater flow, which will be discussed in detail in the next section.

ditional mathematical complexity and less physical clarity. The effect of cohesion is to shift the Coulomb failure curves of Figure 4 upward by an amount $c(\cos \phi)/\gamma_c(\gamma_t - \gamma_w)$, in which c is the cohesion of the soil and γ_c is a critical soil depth required for failure to occur. The liquefaction line of Figure 4 loses its physical significance when cohesion is present, however, because soil with true cohesion cannot lose its strength completely as a result of any seepage condition. For the common case in steep, soil-mantled terrain, in which $\theta \approx \phi$ and a slope is marginally stabilized by a small amount of root strength or cohesion, Figure 4 implies that seepage directed horizontally is most conducive to failure.

ANALYSIS OF STATIC LIQUEFACTION

A static, saturated cohesionless soil mass will liquefy if it experiences a uniform seepage force that has an upward vertical component with a magnitude equal to the submerged unit weight of the soil. In this event the soil becomes strengthless and will deform by flowing rather than by frictional slipping. In terms of the variables of (10) and the geometry of Figure 2, the static liquefaction condition is expressed as

$$z = \cos[(\lambda + \phi) + (\theta - \phi)] = 1 \quad (12)$$

For $z = 1$, (12) is satisfied only if $\lambda = -\theta$, which represents vertically upward seepage. If z is larger than 1, however, (12) may be satisfied for other seepage directions with upward components. These seepage directions are identified by solving (12) for all combinations of λ, θ , and z ; a plot of this solution is presented in Figure 5.

Figure 5 illustrates several important points about liquefaction of static, cohesionless soils on hillslopes. First, the seepage direction can differ significantly from vertically upward, yet static liquefaction can occur with hydraulic gradients not much larger than the normalized critical gradient for upward flow, $z = 1$. For example, seepage that deviates 30° from vertically upward can cause static liquefaction if $z = 1.15$. If the seepage direction deviates further from the vertical than 60° ,

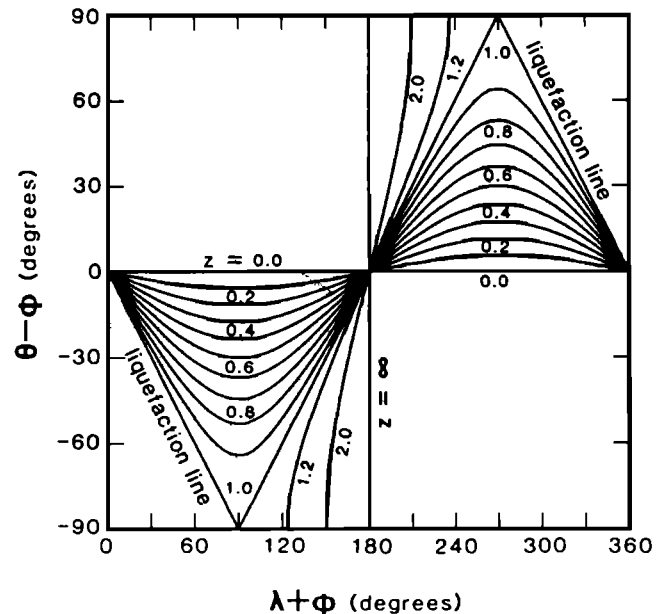


Fig. 4. Universal plot of the normalized limiting stable slope angle as a function of the normalized seepage direction for different values of the normalized seepage magnitude z . Liquefaction preempts Coulomb failure in the zones outside the liquefaction lines.

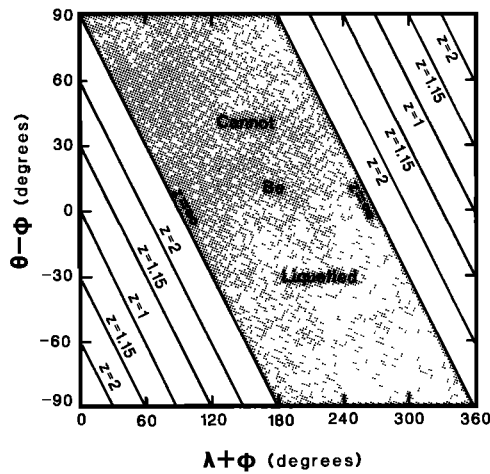


Fig. 5. Values of z required to cause static liquefaction of cohesionless slopes with seepage direction λ and slope angle θ .

however, normalized hydraulic gradients larger than 2 are necessary to cause liquefaction, and liquefaction is impossible if no upward component of seepage exists. From this trend and from the trends for Coulomb failure shown in Figure 4, it appears probable that for many seepage conditions, liquefaction failure will be preempted by Coulomb failure. That is, if seepage conditions were gradually changed through time so that the potential for slope instability were gradually increased, Coulomb failure would precede static liquefaction of the slope. In other instances the converse might be true. In the following section we discuss some typical patterns of seepage in hillslopes and the likelihood of these two modes of failure.

DISCUSSION

The direction of groundwater seepage paths within a saturated slope may vary greatly [Patton and Hendron, 1974; Hodge and Freeze, 1977; Rulon et al., 1985]. Aside from lateral and basal hydrogeologic boundaries, the only significant controls of steady seepage paths are the spatial distribution of topographic potential and soil anisotropy and heterogeneity [cf. Toth, 1963; Freeze and Witherspoon, 1967]. Typical examples of how topographic potential and soil heterogeneities can influence seepage paths in saturated soil-mantled slopes are illustrated by the steady state model results shown in Figures 6 and 7. Figure 6 depicts a flow net that represents a numerical solution of the Laplace equation for flow within a saturated, sloping soil mass that has a hummocky surface. This flow net is intended to represent wet-season groundwater conditions in a persistently unstable, soil-mantled hillslope in

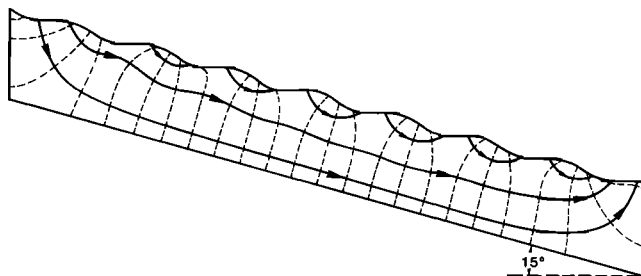


Fig. 6. Numerically computed flow net for steady hillslope seepage influenced by hummocky topography. Hillslope soil prism has a mean length-to-thickness ratio of 8. Sinusoidal hummocks have a wavelength-to-amplitude ratio of 20 and wavelength-to-prism-length ratio of 1/8.

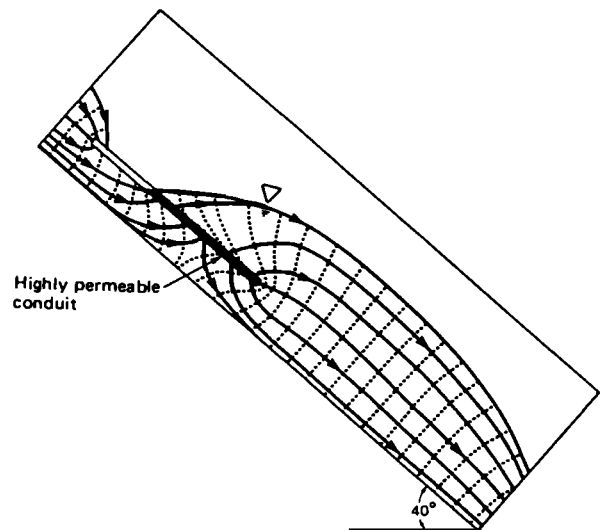


Fig. 7. Hele-Shaw analog results for steady hillslope seepage influenced by a highly permeable conduit (modified from Pierson [1983]). Simulated hydraulic conductivity of the conduit is about 280 times that of the surrounding material. Some flow lines fictitiously appear to converge owing to the finite line thickness.

which $\phi = 20^\circ$ [Iverson, 1986b; R. M. Iverson and J. J. Major, unpublished manuscript, 1986]. The flow net shows the strong asymmetrical influence of topography on seepage directions near the hummocky ground surface. Figure 7 depicts a flow net similar to that constructed by Pierson [1983] on the basis of Hele-Shaw analog model results. This flow net represents seepage in a steep slope that contains a highly permeable subsurface conduit. The two-dimensional flow and effective-stress fields implied by each of these two flow nets are more complex than can be rigorously represented by our analytical results. However, our theory leads us to infer that the weakest regions in each of the model slopes probably occur where the seepage direction is close to horizontal. This inference contrasts markedly with the intuitive interpretation that the weakest regions coincide with the highest water table elevations or with zones of groundwater upflow.

According to Figure 4, the seepage direction most conducive to Coulomb failure is one that makes an acute angle outward from the surface of the slope. Physically, this is the direction that most effectively reduces the slope-normal frictional force while simultaneously enhancing the slope-parallel driving force. In contrast, the seepage direction most effective for liquefying the slope is one that is oriented vertically upward (Figure 5). The disparity between the seepage directions most favorable for Coulomb failure and liquefaction indicates that in most situations one mode of failure will have precedence over the other.

To summarize the diverse slope failure possibilities, Figures 4 and 5 can be superposed to define discrete domains characterized by preferred slope failure modes. For hydraulic gradients that give $z < 1$, Coulomb failure is the only possible mode of slope failure (Figure 4). Many Coulomb failure scenarios are possible, and they constitute the most likely failure mode with typical seepage conditions. Furthermore, comparison of Figures 4 and 5 shows that for seepage directed so that $90^\circ < \lambda < 270^\circ$, the value of z required for Coulomb failure is universally less than the value required for liquefaction of the same slope. Therefore Coulomb failure would preempt liquefaction in such cases. For seepage directed so that $\lambda = -\theta$, the failure lines of Figures 4 and 5 coincide, and Coulomb

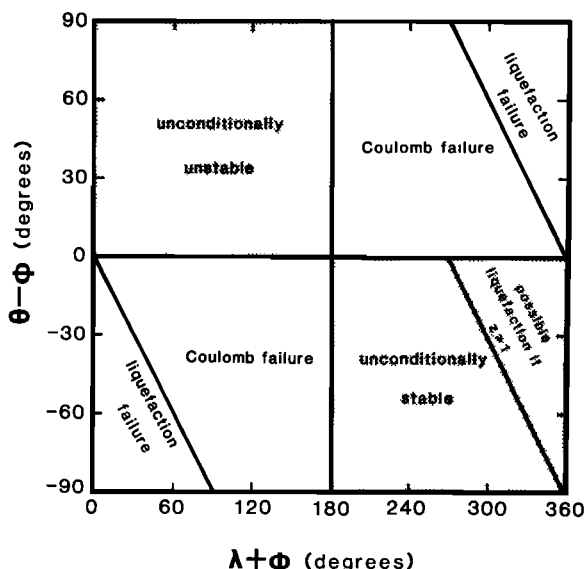


Fig. 8. Distribution of domains that show preferred slope failure mode. The hydraulic gradient is assumed to be large enough to provoke failure, except where slopes are unconditionally stable.

failure and liquefaction occur simultaneously when $z = 1$. Finally, Figures 4 and 5 show that liquefaction is the preferred mode of slope failure in the unlikely circumstance of uphill seepage such that $z > 1$, and either $\lambda + \phi < 90^\circ$ and $\theta < -\lambda$ or $\lambda + \phi > 270^\circ$ and $\theta > -\lambda$. Domains showing all these failure situations are plotted on Figure 8 along with domains that are unconditionally stable or unstable with respect to Coulomb failure. As is shown in Figure 8, liquefaction is possible in a small part of the unconditionally stable domain if z is larger than the values shown in the corresponding domain of Figure 5.

The failure domains of Figure 8 illustrate intriguing possibilities for the initiation of flowing mass movements. In such mass movements (e.g., debris flows), some mechanism such as transient liquefaction is required to explain the transformation of an initially sliding mass into a rapidly deforming flow [Johnson, 1984]. The infinitesimal separation of the liquefaction domains and the Coulomb failure domains of Figure 8 demonstrates that there is a rather slight distinction between Coulomb slip and liquefaction in some failure cases, particularly where there are both a significant upward seepage component and a slope angle nearly equal to ϕ . Coulomb shear failure of a loose soil in these cases could cause transient liquefaction when the soil contracts and interstitial water is forced upward [Sassa, 1984]. Less obvious, perhaps, is the possibility that even a dense soil could liquefy during shear failure if dynamic, shear-induced, pore-pressure perturbations were large enough to cause the effective-stress state to transiently shift from a Coulomb failure domain to a liquefaction domain of Figure 8. The preponderance of natural debris flows that are mobilized in saturated hillslope soil depressions on slopes greater than 30° [e.g., Innes, 1983; Johnson, 1984] lends credence to this idea; convergence of groundwater flow paths in such depressions could produce outward hydraulic gradients during storms, and with $\theta \approx \phi$, soil slips initiated in such depressions might transiently liquefy.

NUMERICAL EXAMPLE

A hypothetical example is presented here as an aid to interpreting Figures 3-5 and 8. Consider a straight, long valley-

side slope that makes an angle of 25° with the horizontal (Figure 9). Assume the soil of the slope is saturated, homogeneous, and cohesionless and has a friction angle $\phi = 30^\circ$ and normalized total unit weight $\gamma_t/\gamma_w = 2$. Figures 3 and 4 show that minimum stability of the slope occurs when $\lambda = 60^\circ$, that is, when seepage is directed outward from the slope at an angle 5° above the horizontal. The slope would undergo Coulomb failure if the hydraulic gradient were about 0.1 in this direction (Figures 3 and 4). Such a condition is quite plausible, but for purposes of illustration, a different case is considered here. If seepage paths make an angle of 30° with the vertical in the potential slope failure zone, as is shown in Figure 9, then $\lambda = 5^\circ$, $\lambda + \phi = 35^\circ$, and $\theta - \phi = -5^\circ$. Figure 5 shows that the slope would liquefy in this situation if the hydraulic gradient, $i (=z$ in this case), were about 1.15. Figures 3 and 4 show that Coulomb failure would occur with a gradient of only about 0.15 in this direction. Thus Coulomb failure takes precedence over liquefaction (compare Figure 8). If, however, soil particle rearrangement during Coulomb failure produced a transient, additional, local hydraulic gradient of 1 in the λ direction, the failing mass would liquefy into a flowing mass.

CONCLUSION

The analysis presented here clarifies some physical effects of groundwater seepage on the potential for slope instability. Although the analysis does not account for complicating circumstances such as soil inhomogeneity or anisotropy or for non-uniformity or temporal variability of the groundwater flow field, the simplicity and generality of the results offer significant insight. The results appear useful particularly in conceptualizing the effects of seepage on slope stability and in interpreting field data and modeling results in a physical context.

A key theme of the analysis presented here is that the seepage force vector, which represents a body force proportional to the hydraulic potential gradient, is responsible for destabilizing hillslopes. We believe the consideration of seepage forces elucidates the physics of the problem more than does the sometimes misleading notion that high pore pressures cause slope instability.

A principal result of the analysis is that if all other factors are constant, minimum slope stability occurs when seepage is directed such that $\lambda = 90^\circ - \phi$. On steep landslide-prone slopes, where the slope angle commonly differs little from ϕ , this result implies that horizontal seepage, as might occur above poorly permeable strata [Rulon et al., 1985], produces minimal slope stability. Another result is that when a verti-

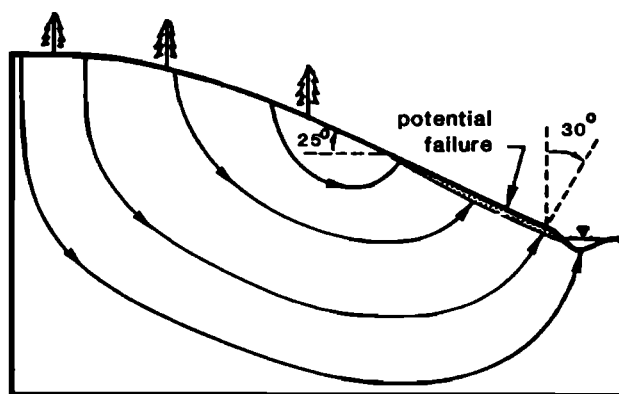


Fig. 9. Hypothetical hillslope showing schematic seepage paths and site of potential slope failure.

cally upward seepage component exists, Coulomb failure may occur under conditions close to those required for static liquefaction. Failure in such instances could catalyze debris flow mobilization.

APPENDIX

To express (3) in terms of pore water pressure gradients it is useful to express the total hydraulic head as the sum of the pressure head and gravitational head

$$h = p/\gamma_w + E$$

in which p is pore water pressure, and E is elevation above an arbitrary horizontal datum. This expression for h neglects other possible contributions to the total hydraulic head, such as those produced by osmosis. Differentiating this expression with respect to the coordinates x and y then gives

$$\frac{\partial h}{\partial y} = \frac{\partial}{\partial y} \left(\frac{p}{\gamma_w} \right) + \frac{\partial E}{\partial y} = \frac{1}{\gamma_w} \frac{\partial p}{\partial y} - \cos \theta$$

$$\frac{\partial h}{\partial x} = \frac{\partial}{\partial x} \left(\frac{p}{\gamma_w} \right) + \frac{\partial E}{\partial x} = \frac{1}{\gamma_w} \frac{\partial p}{\partial x} - \sin \theta$$

Substituting these expressions into (3) yields the stress equilibrium equations in terms of the pore pressure gradients and total unit weight of the soil

$$d\sigma/dy = \gamma_t \cos \theta - \partial p/\partial y$$

$$d\tau/dy = \gamma_t \sin \theta - \partial p/\partial x$$

NOTATION

- c soil cohesion, M/LT^2 .
 E elevation above arbitrary horizontal datum, L .
 f seepage force per unit volume, M/L^2T^2 .
 g gravitational acceleration, L/T^2 .
 g magnitude of gravitational acceleration, L/T^2 .
 h total hydraulic head of pore water, L .
 i magnitude of hydraulic gradient vector (dimensionless).
 K hydraulic conductivity, L/T .
 p pore-water pressure, M/LT^2 .
 q specific discharge, L/T .
 T effective stress tensor, M/LT^2 .
 x, y orthogonal coordinate directions, L .
 y_c value of y at which failure occurs if nonzero cohesion is present, L .
 z ratio of seepage force magnitude to submerged unit weight of soil (dimensionless).
 γ_b buoyant unit weight of soil, M/L^2T^2 .
 γ_t total unit weight of soil, M/L^2T^2 .

- γ_w unit weight of water, M/L^2T^2 .
 θ surface slope angle.
 λ angle of seepage vector measured clockwise from outward directed surface-normal vector.
 ρ_t total soil bulk density, M/L^3 .
 ρ_w pore water density, M/L^3 .
 σ effective normal stress, M/LT^2 .
 τ shear stress, M/LT^2 .
 ϕ internal friction angle of soil.

Acknowledgments. We thank B. Voight and J. Bredehoeft for reviewing a preliminary version of this paper.

REFERENCES

- Bear, J., *Dynamics of Fluids in Porous Media*, Elsevier Science, New York, 1972.
Dwight, H. B., *Tables of Integrals and Other Mathematical Data*, MacMillan, New York, 1961.
Freeze, R. A., and P. A. Witherspoon, Theoretical analysis of regional groundwater flow, 2, Effect of water table configuration and subsurface permeability variation, *Water Resour. Res.*, 3, 623-634, 1967.
Hodge, R. A. L., and R. A. Freeze, Groundwater flow systems and slope stability, *Can. Geotech. J.*, 14, 466-476, 1977.
Innes, J. L., Debris flows, *Prog. Phys. Geogr.*, 7, 469-501, 1983.
Iverson, R. M., Unsteady, nonuniform landslide motion, 1, Theoretical dynamics and the steady datum state, *J. Geol.*, 94, 1-15, 1986a.
Iverson, R. M., Dynamics of slow landslides: A theory for time-dependent behavior, in *Hillslope Processes*, edited by A. D. Abrahams, pp. 297-317, Allen and Unwin, Winchester, Mass., 1986b.
Johnson, A. M., Debris flow, in *Slope Instability*, edited by D. Brunsten and D. B. Prior, pp. 257-361, John Wiley, New York, 1984.
Lambe, T. W., and R. V. Whitman, *Soil Mechanics*, John Wiley, New York, 1979.
Patton, F. D., and A. J. Hendron, General report on mass movements, in *Proceedings 2nd International Congress*, vol. 2, V-GR-1-57, International Association Engineering Geologists, Sao Paulo, Brazil, 1974.
Pierson, T. C., Soil pipes and slope stability, *Q. J. Eng. Geol.*, 16, 1-11, 1983.
Rulon, J. J., R. Rodway, and R. A. Freeze, The development of multiple seepage faces on layered slopes, *Water Resour. Res.*, 21, 1625-1636, 1985.
Sassa, K., The mechanism starting liquefied landslides and debris flows, in *Proceedings of the 4th International Conference on Landslides*, pp. 349-354, vol. 2, University of Toronto Press, Downview, Ont., 1984.
Toth, J., A theoretical analysis of groundwater flow in small drainage basins, *J. Geophys. Res.*, 68, 4795-4812, 1963.

R. M. Iverson and J. J. Major, U.S. Geological Survey, David A. Johnston Cascades Volcano Observatory, 5400 MacArthur Boulevard, Vancouver, Washington 98661.

(Received January 30, 1986;
revised June 3, 1986;
accepted June 4, 1986.)